JOURNAL OF SOLID STATE CHEMISTRY **13**, 107–113 (1975)

# Some Thermodynamic Properties in Spinel Solid Solutions with the $Fe_3O_4$ Component

TAKASHI KATSURA, MASATAKA WAKIHARA, SHIN-ICHI HARA, AND TADASHI SUGIHARA

*Department of Chemistry, Tokyo Institute of Technology, Ookayama, Meguro-ku, Tokyo, Japan*

Received March 1, 1974

Phase equilibria in Fe–$Fe_2O_3$–$Cr_2O_3$, Fe–$Fe_2O_3$–$V_2O_3$, FeO–$Fe_2MoO_4$–$Fe_3O_4$, and FeO–$Fe_2O_3$–$ZrO_2$ systems were precisely determined. On the basis of the present results, together with the FeO–$Fe_2O_3$–$TiO_2$ system studied by Taylor at 1300°C and by Webster and Bright at 1200°C, the following results were obtained. (1) The solid solutions $Fe_2TiO_4$–$Fe_3O_4$, and $Fe_2MoO_4$–$Fe_3O_4$ are approximately ideal in respect to the activity–composition relation. (2) On the contrary, the solid solutions $FeCr_2O_4$–$Fe_3O_4$ and $FeV_2O_4$–$Fe_3O_4$ deviate significantly from Raoult's law, and these are of regular solution defined by Hildebrand.

## Introduction

Phase equilibria in the FeO–$Fe_2O_3$–$TiO_2$ system were studied by Taylor (*1*) at 1300°C, and by Webster and Bright (*2*) at 1200°C. According to them, the wüstite phase contains no appreciable amount of $TiO_2$, and pure wüstite is directly in equilibrium with the stoichiometric spinel phase. Phase equilibria in the FeO–$Fe_2O_3$–$MoO_2$ was partly studied by Abe (*3*), and he prepared the stoichiometric $Fe_2MoO_4$ which is an inverse spinel. However, he only estimated roughly oxygen isobaric lines in the field of spinel + wüstite. On the other hand, the wüstite phase in the FeO–$Fe_2O_3$–$Cr_2O_3$ system at 1300°C (*4*) and in the FeO–$Fe_2O_3$–$V_2O_3$ system at 1500 K (*5*) contains significant amounts of $Cr_2O_3$ and $V_2O_3$, respectively. Schmahl and Dillenburg (*6*) studied the phase equilibria in the Fe–Cr–O and Fe–V–O system at 900°C, and they calculated some free energy values. Activities of components in the spinel solid solutions calculated by them were obtained without considering the existence of the ternary wüstite solid solutions.

In the present paper, we will present precise phase equilibria in the Fe–$Fe_2O_3$–$Cr_2O_3$, Fe–$Fe_2O_3$–$V_2O_3$, FeO–$Fe_3O_4$–$Fe_2MoO_4$, and FeO–$Fe_2O_3$–$ZrO_2$ systems in order to calculate the activity of the component $Fe_3O_4$ in each spinel solid solution.

We omitted the activity calculation for the spinel phase containing $ZrO_2$, because the solubility of $ZrO_2$ in the magnetite phase was so small. The activity of the $Fe_3O_4$ component in the $Fe_3O_4$–$Fe_2TiO_4$ solid solution was calculated by using the data obtained by Taylor (*1*), and Webster and Bright (*2*).

## Experimental

### *Materials*

We used $V_2O_5$, $Fe_2O_3$, $Cr_2O_3$, $MoO_2$, and $ZrO_2$ to prepare starting materials. We obtained $V_2O_5$ by decomposing guaranteed reagent grade ammonium metavanadate at 450°C in air. Analytical grades of $Fe_2O_3$, $Cr_2O_3$, and $ZrO_2$ were dried in air at 700°C. $MoO_2$ was obtained by decomposing guaranteed reagent grade $MoO_3$ in a mixed gas with a ratio $CO_2/H_2 = 1$ at 600°C for 2 hr. Thus obtained, $MoO_2$ was heated again in the same atmosphere at 1100°C for 5 hr, then quenched. Chemical analysis showed that $MoO_2$ thus obtained has the stoichiometric composition. Mixtures of desired $Fe_2O_3/V_2O_5$, $Fe_2O_3/MoO_2$, $Fe_2O_3/Cr_2O_3$, and $Fe_2O_3/ZrO_2$ ratios were prepared by grinding repeatedly in an agate mortar under ethyl alcohol. Then, mixtures of $Fe_2O_3/V_2O_5$ were pressed loosely in a small-size alumina crucible, and heated at 650°C in the mixed gas with a ratio $CO_2/H_2 = 1$ for 1 hr. After quenching, the sintered sample was crushed to obtain small size pieces ($3 \times 3 \times 3$ mm$^3$). Mixtures of $Fe_2O_3/MoO_2$ were heated at 600°C for 2 hr in a mixed gas with a ratio of $CO_2/H_2 = 1$, then heated again at 1100°C for 30 min in the same atmosphere in order to obtain the sintered pieces. Mixtures of desired $Fe_2O_3/Cr_2O_3$ and $Fe_2O_3/ZrO_2$ were heated at 1200°C in air.

*Procedures*

About 3 *g* of small-size pieces having a desired composition were put into an alumina crucible which had slit-cuts on the wall and the bottom in order to facilitate equilibration between the solid and the gas phases. The crucible was suspended in a vertical furnace, and subsequent thermogravimetric procedures were the same as those described in previous papers (*4*, *7*). Solid solutions with stoichiometric compositions were chosen as the reference for sample weight.

The thermocouple, Pt-13%Rh87%Pt, was calibrated against the melting point of gold, and the fluctuation of temperature at the point where a sample was set inside the furnace was within ±1°C. Partial pressures of oxygen inside the furnace were measured by means of the solid electrolyte cell composed of $(ZrO_2)_{0.85}(CaO)_{0.15}$. The differences between measured and calculated partial pressures of oxygen were within $\pm 0.01$ in terms of $\log P_{O_2}$ in the range $10^{-9}$–$10^{-13}$ atm $P_{O_2}$. The procedure to measure the partial pressure of oxygen has been described in a previous paper (*7*).

## Results and Discussion

### (*1*) *Phase Equilibria*

Figure 1 shows the phase equilibria in the $Fe$–$Fe_2O_3$–$Cr_2O_3$ system at 1500 K. As seen in Fig. 1, the $Fe_3O_4$–$FeCr_2O_4$ solid solution extends to a point *A*. This chromite *A* is stable against an aqueous solution of HCl, and thus, it was easily separated from the coexisting metallic iron which contained a negligible amount of Cr. The powder X-ray diffraction pattern showed an identical structure with that of the stoichiometric $FeCr_2O_4$, with the cell dimension of 8.383 Å which is larger than that of stoichiometric $FeCr_2O_4$, 8.374 Å. The solid solution from $Fe_3O_4$ to a point *B* in Fig. 1 is in equilibrium with chromian wüstite, *C*–*E*, and the solid solution from *B* to chromite *A* is in equilibrium with metallic iron.

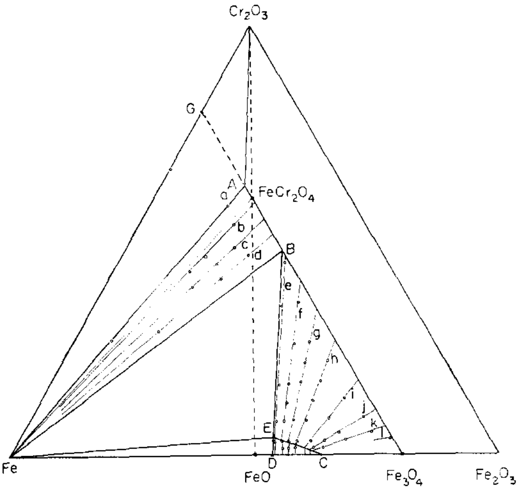

FIG. 1. Phase equilibria in the $Fe$–$Fe_2O_3$–$Cr_2O_3$ system at 1500 K. Heavy lines are boundary curves, light lines are oxygen isobars. The $-\log P_{O_2}$ value of each light line is as follows: $a = 13.97$, $b = 12.42$, $c = 11.94$, $d = 11.78$, $B = 11.60$, $e = 11.53$, $f = 10.99$, $g = 10.58$, $h = 10.12$, $i = 9.60$, $j = 9.92$, $k = 9.09$, and $Fe_3O_4 = 8.60$. Compositions are expressed in mole%: *A*, 17.40% $Fe_2O_3$, 19.60% Fe, 63.00% $Cr_2O_3$; *B*, 32.48% $Fe_2O_3$, 20.00% Fe, 47.52% $Cr_2O_3$; *C*, 63.89% $Fe_2O_3$, 36.11% Fe; *D*, 53.73% $Fe_2O_3$, 46.27% Fe; *E*, 51.73% $Fe_2O_3$, 44.09% Fe, 4.18% $Cr_2O_3$.

Figure 2 shows the phase equilibria in the $Fe$–$Fe_2O_3$–$V_2O_3$ system at 1500 K. The solid solution from $Fe_3O_4$ to a point *B* is in equilibrium with vanadowüstite, *C*–*E*, and the solid solution from *B* to $FeV_2O_4$ is in equilibrium with metallic iron. The general features found in this system are quite similar to that of the $Fe$–$Fe_2O_3$–$Cr_2O_3$ system.

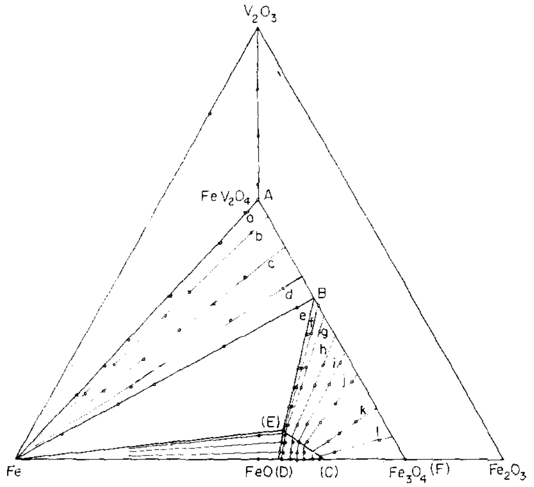

FIG. 2. Phase equilibria in the Fe–$Fe_2O_3$–$V_2O_3$ system at 1500 K. The $-\log P_{O_2}$ value of each light line is as follows: $a = 13.45, b = 12.69, c = 12.20, d = 11.87, e = 11.68, f = 11.56, g = 11.37, h = 10.83, i = 10.45, j = 10.03, k = 9.39$, and $l = 8.98$. Composition are expressed in mole%: $B$, 42.80% $Fe_2O_3$, 20.00% Fe, 37.20% $V_2O_3$; $E$, 51.60% $Fe_2O_3$, 41.70% Fe, 6.70% $V_2O_3$.

Figure 3 shows the phase equilibria in the $Fe_3O_4$–$Fe_2MoO_4$–FeO system. The number attached to the oxygen isobars mean the $-\log P_{O_2}$ value. As seen in Fig. 3, the $Fe_2MoO_4$–$Fe_3O_4$ solid solution is directly in equilibrium with binary solid solution of wüstite, and the general features are similar to that of the $Fe_3O_4$–$Fe_2TiO_4$–FeO found by Taylor (*1*) and Webster and Bright (*2*). On the basis of the present data, we prepared stoichiometric $Fe_2MoO_4$–$Fe_3O_4$ solid solutions with desired compositions, and obtained the relationship between the cell constant and composition. Table I gives the results. From the data of Table I, it is clear that the cell constant is proportional to the composition.

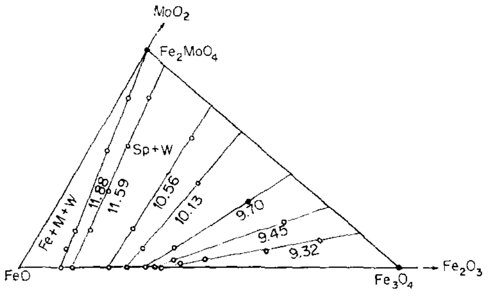

FIG. 3. Phase equilibria in the $Fe_3O_4$–$Fe_2MoO_4$–FeO system at 1200°C. The number attached to the oxygen isobars mean the $-\log PO_2$ value. Abbreviations used have the following meanings: Sp, spinel solid solution; W, wüstite; Fe, metallic iron.

TABLE I

THE RELATIONSHIP BETWEEN CELL CONSTANT AND COMPOSITION OF SPINEL SOLID SOLUTIONS

| $N_{Fe_3O_4}$ | $a_0$ (Å) (±0 001) |
|---|---|
| $Fe_2MoO_4$–$Fe_3O_4$ | |
| 1 | 8.396 |
| 0.842 | 8.414 |
| 0.667 | 8.433 |
| 0.471 | 8.455 |
| 0.250 | 8.480 |
| 0 | 8.509 |
| Limited solid solution of $Fe_2ZrO_4$–$Fe_3O_4$ | |
| 1 | 8.396 |
| 0.970 | 8.408 |
| 0.954 | 8.413 |
| 0.939 | 8.417 |
| 0.935 (point *C*) | 8.419 |

Figure 4 shows the phase equilibria in the FeO–$Fe_2O_3$–$ZrO_2$ system at 1200°C. As seen in Fig. 4, there appeared a limited ternary spinel solid solution *C–D–F* where the phase boundary *C–F* is supposed to be on the $Fe_2ZrO_4$(*Z*)–$Fe_3O_4$(*F*) line. Thus, if we imagine a nonexisting compound $Fe_2ZrO_4$, magnetite can dissolve about 6 ± 1 mole% $Fe_2ZrO_4$. The spinel solid solution on the *C–D* line is in equilibrium with $ZrO_2$. In the present study, we could not clarify the solubility of iron oxide in $ZrO_2$. The spinel solid solution on the *C–F* line is in equilibrium with wüstite solid solution *B–B′*. The wüstite solid solution *A–B* is in equilibrium with $ZrO_2$. The composition of each point is given in Fig. 4. On the basis of the present data, we prepared four stoichiometric solid solutions on the *C–F* line, and determined the cell constant. The results are given in Table I.

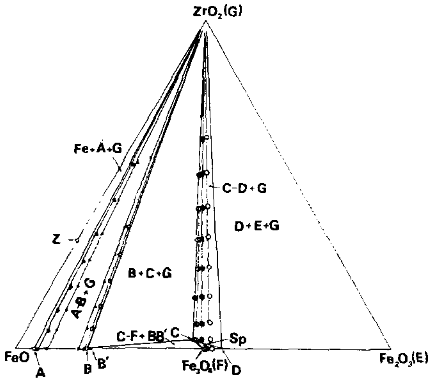

FIG. 4. Phase equilibria in the $FeO–Fe_2O_3–ZrO_2$ system at 1200°C. Symbols have the following meanings: ○ at $10^{-3.76}$ atm $P_{O_2}$; ● at $10^{-7.98}$ atm $P_{O_2}$; ⊙ at $10^{-9.09}$ atm $P_{O_2}$; ⊕ at $10^{-9.16}$ atm $P_{O_2}$; ○ at $10^{-9.21}$ atm $P_{O_2}$; × at $10^{-9.60}$ atm $P_{O_2}$; ▲ at $10^{-11.32}$ atm $P_{O_2}$; ● at $10^{-11.82}$ atm $P_{O_2}$. Abbreviations have the following meanings: *G*, $ZrO_2$; *E*, $Fe_2O_3$; *F*, stoichiometric $Fe_3O_4$; *D*, magnetite with a composition 0.546 FeO, 0.454 $Fe_2O_3$ in mole fraction; *B′*, wüstite in equilibrium with (*F*) having a composition, 0.198 $Fe_2O_3$, 0.802 FeO in mole fraction; *B*, wüstite in equilibrium with spinel *C* having a composition, 0.027 $ZrO_2$, 0.515 FeO, 0.458 $Fe_2O_3$; *A*, wüstite in equilibrium with metallic iron having a composition, 0.948 FeO, 0.052 $Fe_2O_3$ in mole fraction; *Z*, nonexisting $Fe_2ZrO_4$.

### (2) *Calculation of the Activity of the $Fe_3O_4$ Component in Spinel Solid Solutions*

Darken and Schwerdtfeger (*8*) have shown that the atomistic assumptions for ideal mixing in solid solutions of the type $A_uX_v - B_uX_v$ lead to expression,

$$a_{B_uX_v} = (N_{B_uX_v})\,u$$

where *a* means activity and *N* means mole fraction. That is, the solution will follow Raoult's law if one chooses as components $AX_{v/u}$ and $BX_{v/u}$ to form one gram atom of species being mixed. In the systems, $Fe_2TiO_4$–$Fe_3O_4$ and $Fe_2MoO_4$–$Fe_3O_4$, since one mole of Mo or Ti is substituting one mole of Fe, the proper choice of components for assessing the ideal behavior would be $Fe_3O_4$, $Fe_2TiO_4$, and $Fe_2MoO_4$. On the contrary, in the $FeCr_2O_4$–$Fe_3O_4$ and the $FeV_2O_4$–$Fe_3O_4$ systems, one is substituting two moles of Cr or V for two moles of Fe, and the proper choice of components would be $Fe^{2+}_{0.5}CrO_2$, $Fe^{2+}_{0.5}VO_2$, and $Fe^{2+}_{0.5}Fe^{3+}O_2$ rather than $FeCr_2O_4$, $FeV_2O_4$, and $Fe_3O_4$. Then, we would obtain the following relation,

$$a_{Fe^{2+}_{0.5}Fe^{3+}O_2} = (a_{Fe_3O_4})^{1/2}. \qquad (1)$$

Under these considerations of atomistic assumption, the activity of the $Fe_3O_4$ component for the systems $Fe_2TiO_4$–$Fe_3O_4$ and $Fe_2MoO_4$–$Fe_3O_4$ may be calculated from the following equations.

$$3\ Fe + 2\,O_2 = Fe_3O_4 \qquad (2)$$

$$\log a_{Fe_3O_4} = \log K + 2 \log P_{O_2} + 3 \log a_{Fe}, \qquad (3)$$

where *K* is the equilibrium constant in Eq. (2), and where *a* means the activity of each chemical species. In the present study, we determined the values of log *K* at 1500 K and 1200°C to be 22.175 and 22.915, respectively. These values are identical with those obtained by Darken and Gurry (*9*) (22.19 at 1500 K and 22.922 at 1200°C). Here, we will use the present values of log K for determining the $Fe_3O_4$ activity. The activity of $Fe^{2+}_{0.5}Fe^{3+}O_2$ for the systems $FeCr_2O_4$–$Fe_3O_4$ and $FeV_2O_4$–$Fe_3O_4$ will be calculated on the basis of Eq. (1).

Since the $Fe_2MoO_4$–$Fe_3O_4$ and the $Fe_2TiO_4$–$Fe_3O_4$ solid solutions are in equilibrium with pure wüstite solid solution, $a_{Fe_3O_4}$ in these solid solutions is readily calculated on the basis of the activity of Fe in the wüstite solid solution. In cases of the $FeCr_2O_4$–$Fe_3O_4$ and the $FeV_2O_4$–$Fe_3O_4$ solid solutions, partial solid solution from $FeCr_2O_4$ or $FeV_2O_4$ to a point *B* are in equilibrium with metallic iron. Thus, the $a_{Fe^{2+}_{0.5}Fe^{3+}O_2}$ is readily calculated. However, partial solid solutions from *B* to $Fe_3O_4$ are in equilibrium with ternary wüstite solid solutions having compositions on the *C–E* line. Thus, $a_{Fe^{2+}_{0.5}Fe^{3+}O_2}$ in spinel solid solutions ranging from *B* to $Fe_3O_4$ in both systems may be evaluated from $a_{Fe}$ on the *C–E* line and by using Eq. (3). The *C–E* lines in both Figs. 1 and 2 were determined experimentally on the basis of intersections of the isobaric lines of oxygen. In the present study, we calculated the activity of metallic iron on the *C–E* line by applying the method developed by Schuhmann (*10*). The integrations in

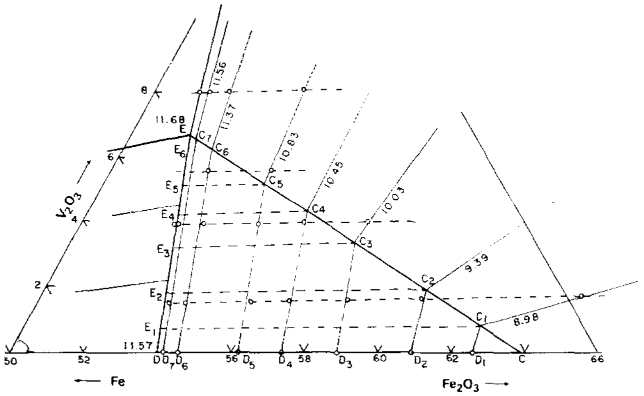

FIG. 5. Detailed figure of wüstite field in the $Fe$–$Fe_2O_3$–$V_2O_3$ system at 1500 K for interpreting the integration of Schuhmann's method.

Schuhmann's method are performed by the following Eq. (4),

$$\left[\log a_{Fe}(C_i') = \log a_{Fe}(E_i) - 1/2 \int_{\log P_{O_2}(E_i)}^{\log P_{O_2}(C_i')} (\delta n_O/\delta n_{Fe})_{a_O, n_M} d \log P_{O_2}\right]_{n_{Fe}/n_M} \quad (4)$$

where $a_{Fe}(C_i')$ means an activity of metallic iron in any point having a composition within the ternary wüstite field, and where $a_{Fe}(E_i)$ means an activity of metallic iron just on the $D$–$E$ line having a composition $E_i$. Since wüstite with a composition on the $D$–$E$ line is in equilibrium with metallic iron, $a_{Fe}(E_i)$ is unity. The composition $C_i'$ must have the same $n_{Fe}/n_{(\mathrm{Cr\ or\ V})}$ ratio with that of $E_i$. As an example, a detailed figure of the ternary wüstite field in the $Fe$–$Fe_2O_3$–$V_2O_3$ system is given in Fig. 5. Here, $C_2'$ is any composition on the $E_2$–$C_2$ line which shows a constant $n_{Fe}/n_V$. Because the isobaric oxygen pressure curve in the wüstite field is substantially straight, the partial derivative $(\delta n_O/\delta n_{Fe})_{aO, n_V}$ is evaluated by a point $D_2$ which corresponds to the composition of wüstite on the $C$–$D$ line. By integrating from $E_2$ to $C_2$, we determine the activity of Fe at a point of $C_2$ on the $C$–$E$ line. The $a_{Fe}$ thus obtained is used to calculate the $a_{Fe^{2+}Fe^{+3}O_2}$ of the spinel solid solution by applying Eq. (3). Numerical values to calculate the $a_{Fe_3O_4}$ and $a_{Fe^{2+}_{0.5}Fe^{3+}O_2}$ of the stoichiometric spinel solid solutions are listed in Tables II and III, respectively. Figure 6 shows the relationship between activity and composition for the four spinel solid solutions. The spinel solid solution found in the $FeO$–$Fe_2O_3$–$ZrO_2$ system ranged only from $Fe_3O_4$ to about 6 mole% $Fe_2ZrO_4$, and we omitted the activity calculation.

TABLE II

THE RELATIONSHIP BETWEEN ACTIVITY AND COMPOSITION FOR THE $Fe_2MoO_4$–$Fe_3O_4$ AND THE $Fe_2TiO_4$–$Fe_3O_4$ SYSTEMS

| $N_{Fe_3O_4}$ | $-\log P_{O_2}$ (atm) | $-\log a_{Fe}$ | $a_{Fe_3O_4}$ |
|---|---|---|---|
| | $Fe_2MoO_4$–$Fe_3O_4$ (at 1200°C) | | |
| 1 | 9.14 | 1.545 | 1 |
| 0.887 | 9.32 | 1.440 | 0.902 |
| 0.795 | 9.46 | 1.371 | 0.804 |
| 0.664 | 9.70 | 1.232 | 0.668 |
| 0.473 | 10.13 | 1.000 | 0.452 |
| 0.340 | 10.56 | 0.762 | 0.327 |
| 0.125 | 11.59 | 0.191 | 0.145 |
| | $Fe_2TiO_4$–$Fe_3O_4$ (at 1300°C, by Taylor (*1*)) | | |
| 0.73 | 8.00 | 1.52 | 0.77 |
| 0.59 | 8.62 | 1.14 | 0.61 |
| 0.31 | 9.57 | 0.62 | 0.28 |
| 0.20 | 10.28 | 0.24 | 0.15 |
| 0.15 | 10.63 | 0.06 | 0.10 |
| | $Fe_2TiO_4$–$Fe_3O_4$ (at 1200°C, by Webster and Bright (*2*)) | | |
| 0.88 | 9.32 | 1.44 | 0.92 |
| 0.43 | 10.60 | 0.72 | 0.38 |
| 0.31 | 10.79 | 0.61 | 0.33 |
| 0.22 | 11.54 | 0.21 | 0.16 |

As seen in Fig. 6, the spinel solid solutions of $Fe_2TiO_4$–$Fe_3O_4$ and $Fe_2MoO_4$–$Fe_3O_4$ seem to

TABLE III

THE RELATIONSHIP BETWEEN ACTIVITY AND COMPOSITION FOR THE $Fe_3O_4$–$FeV_2O_4$ AND $Fe_3O_4$–$FeCr_2O_4$ TOGETHER WITH SOME RELATED VALUES

| | Wüstite field | | | | | | | Spinel solid solution | | | |
|---|---|---|---|---|---|---|---|---|---|---|---|
| | Composition of wüstite on C–E line equilibrated with spinel (mole) $Fe_2O_3$ | Fe | $V_2O_3(Cr_2O_3)$ | $-\log P_{O_2}$ on C–E line (atm) | $-\log P_{O_2}$ on E–D line with the same ratio Fe/(V or Cr) | $(\delta n_O/\delta n_{Fe})_{a_O}$ | $-\log a_{Fe}$ on C–E line | $N_{Fe_3O_4}$ in spinel | $-\log P_{O_2}$ on spinel | $a_{Fe_{0.5}^{2+}Fe^{3+}O_2}$ | $\alpha$ |
| | Vanadowüstite | | | | | | | | | | |
| $C$ | 63.9 | 36.1 | 0.0 | 8.68 | 11.57 | 1.170 | 1.605 | 1 | 8.68 | 1 | — |
| $C_1$ | 62.4 | 36.8 | 0.0 | 8.98 | 11.58 | 1.154 | 1.433 | 0.913 | 8.98 | 0.913 | — |
| $C_2$ | 60.4 | 37.7 | 1.9 | 9.39 | 11.60 | 1.138 | 1.210 | 0.805 | 9.39 | 0.767 | −0.553 |
| $C_3$ | 57.7 | 38.9 | 3.4 | 10.03 | 11.62 | 1.113 | 0.861 | 0.672 | 10.03 | 0.585 | −0.559 |
| $C_4$ | 55.9 | 39.8 | 4.3 | 10.45 | 11.64 | 1.094 | 0.638 | 0.590 | 10.45 | 0.481 | −0.528 |
| $C_5$ | 54.4 | 40.4 | 5.2 | 10.83 | 11.66 | 1.079 | 0.442 | 0.525 | 10.83 | 0.395 | −0.548 |
| $C_6$ | 52.4 | 41.4 | 6.2 | 11.37 | 11.67 | 1.058 | 0.158 | 0.438 | 11.37 | 0.303 | −0.507 |
| $E$ | 51.6 | 41.7 | 6.7 | 11.68 | 11.68 | 1.052 | 0 | 0.373 | 11.68 | 0.246 | −0.459 |
| | | | | | | | | 0.295 | 11.87 | 0.166 | −0.502 |
| | | | | | | | | 0.180 | 12.20 | 0.077 | −0.549 |
| | | | | | | | | 0.065 | 12.69 | 0.025 | −0.475 |
| | Chromian wüstite | | | | | | | | | | |
| $C$ | 63.9 | 36.1 | 0.0 | 8.68 | 11.57 | 1.170 | 1.605 | 1 | 8.68 | 1 | — |
| $C_1$ | 61.6 | 37.6 | 0.8 | 9.09 | 11.575 | 1.367 | 1.367 | 0.893 | 9.09 | 0.890 | — |
| $C_2$ | 60.6 | 38.2 | 1.2 | 9.29 | 11.58 | 1.1424 | 1.253 | 0.838 | 9.29 | 0.832 | — |
| $C_3$ | 59.5 | 38.9 | 1.6 | 9.60 | 11.58 | 1.1297 | 1.080 | 0.713 | 9.60 | 0.742 | +0.210 |
| $C_4$ | 57.3 | 40.4 | 2.3 | 10.12 | 11.585 | 1.1084 | 0.790 | 0.560 | 10.12 | 0.609 | +0.188 |
| $C_5$ | 55.5 | 41.5 | 3.0 | 10.58 | 11.59 | 1.0892 | 0.541 | 0.432 | 10.58 | 0.500 | +0.197 |
| $C_6$ | 53.9 | 42.6 | 3.5 | 10.99 | 11.595 | 1.0720 | 0.321 | 0.330 | 10.99 | 0.416 | +0.224 |
| $C_7$ | 52.4 | 43.6 | 4.0 | 11.53 | 11.60 | 1.0540 | 0.037 | 0.225 | 11.53 | 0.331 | +0.279 |
| $E$ | 52.1 | 43.7 | 4.2 | 11.60 | 11.60 | 1.0520 | 0 | 0.208 | 11.60 | 0.306 | +0.267 |
| | | | | | | | | 0.142 | 11.78 | 0.203 | +0.210 |
| | | | | | | | | 0.085 | 11.94 | 0.122 | +0.187 |
| | | | | | | | | 0.025 | 12.42 | 0.047 | +0.288 |

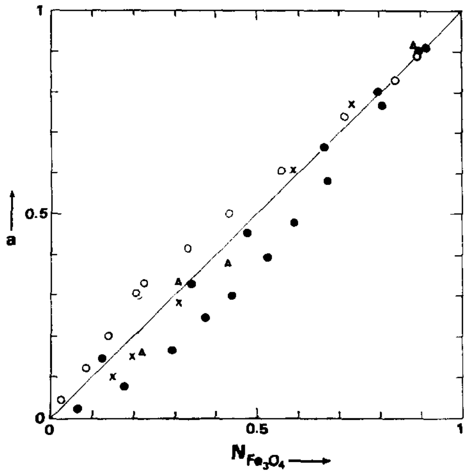

FIG. 6. The relationship between activity and composition. Symbols used have the following meanings: o $FeCr_2O_4$–$Fe_3O_4$; ● $FeV_2O_4$–$Fe_3O_4$; ⊕ $Fe_2MoO_4$–$Fe_3O_4$; x $Fe_2TiO_4$–$Fe_3O_4$ at 1300°C by Taylor, and △ at 1200°C by Webster and Bright.

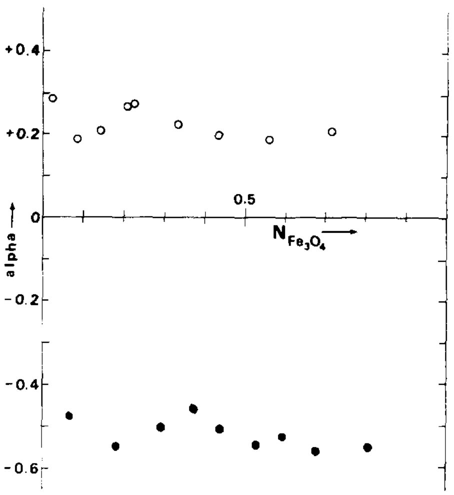

FIG. 7. The relationship between α-function and composition. Symbols have the same meanings as those in Fig. 6.

be nearly ideal in respect to the activity–composition relation. On the contrary, the spinel solid solution of $FeCr_2O_4$–$Fe_3O_4$ shows significantly a positive deviation from Raoult's law, and that of $FeV_2O_4$–$Fe_3O_4$ negative. Such a nonideality found in spinel solid solutions will be characterized by the α-function [$\alpha = \log \gamma_{Fe^{2+}_{0.5}Fe^{3+}O_2}/(1 - N_{Fe_3O_4})^2$]. Figure 7 shows the relationship between $\alpha$ and $N_{Fe_3O_4}$ in the $FeCr_2O_4$–$Fe_3O_4$ and the $FeV_2O_4$–$Fe_3O_4$ solid solutions at 1500 K. It is clear from Fig. 7 that the α-function seems to be constant within the present experimental errors, and thus, these solid solutions may behave as a regular solution defined by Hildebrand (*11*).

## Acknowledgment

We express our thanks to Professor A. Navrotsky, Arizona State University.

## References

1. R. W. TAYLOR, *Amer. Mineral.* **49**, 1016 (1964).
2. A. H. WEBSTER AND N. F. H. BRIGHT, *J. Amer. Ceram. Soc.* **44**, 110 (1961).
3. M. ABE, *Mater. Res. Bull.* **7**, 1443 (1972).
4. T. KATSURA AND A. MUAN, *Trans. AIME* **230**, 77 (1964).
5. M. WAKIHARA AND T. KATSURA, *Bull. Chem. Soc. Japan* **44**, 3043 (1971).
6. G. SCHMAHL AND H. DILLENBURG, *Z. Phys. Chem.* **65**, 119 (1969).
7. T. KATSURA AND M. HASEGAWA, *Bull. Chem. Soc. Japan* **40**, 561 (1967).
8. L. S. DARKEN AND K. SCHWERDTFEGER, *Trans. AIME* **236**, 208 (1966).
9. L. S. DARKEN AND R. W. GURRY, *J. Amer. Chem. Soc.* **67**, 1398 (1945).
10. R. SCHUHMANN, JR., *Acta Met.* **3**, 219 (1955).
11. J. H. HILDEBRAND, *J. Amer. Chem. Soc.* **51**, 66 (1929).